

A rational structure-based drug design strategy for the discovery of novel antiviral agents against the Yellow Fever Virus helicase

Eleni Papakonstantinou¹, Katerina Pierouli¹, George N Goulielmos², Elias Eliopoulos¹✉

¹Laboratory of Genetics, Department of Biotechnology, School of Applied Biology and Biotechnology, Agricultural University of Athens, Athens, Greece

²Section of Molecular Pathology and Human Genetics, Department of Internal Medicine, School of Medicine, University of Crete, Heraklion, Greece

Competing interests: EP none; KP none; GNG none; EE none

Abstract

Yellow Fever is a viral hemorrhagic disease that is transmitted mainly through arthropods with high mortality rates. Yellow Fever Virus (YFV) is an enveloped positive sense single-stranded RNA virus, member of the *Flaviviridae* family and the *Flavivirus* genus, and is endemic in countries of Africa and South America. However, recent cases of infection in North America, Asia and Europe are highlighting the potential risk of an outbreak with no effective treatment available and the urgent need to develop potent antiviral agents against the YFV. In this direction, a range of specific modulators were designed and *in silico* evaluated in an effort to hinder the enzymatic activity of the YFV helicase as a prominent pharmacological target. Following a structure-based rational drug design pipeline, a phylogenetic analysis of *Flaviviridae* viruses and an in-depth evolutionary study on the Yellow Fever Virus helicase has provided invaluable insights into structural conservation and structural elements and features that are vital for the viral helicase function. Using comparative modelling and molecular dynamics simulations the YFV helicase-ssRNA complex was established, and the specific molecular interactions and physicochemical properties of the complex could be analyzed and used towards the designing and elucidation of a specific YFV 3D pharmacophore model. A high throughput virtual screening simulation was conducted to assess a set of in-house maintained low molecular weight compounds as bioactive inhibitors of the YFV helicase enzyme. The *in-silico* study described herein, could pave the way towards the designing and more efficient screening of potential novel modulator compounds against the YFV as well as attest and designate the NS3 helicase as an antiviral pharmacological target of uttermost value and potential.

Introduction

The viral family *Flaviviridae* comprises the genera *Flavivirus*, *Hepacivirus*, *Pestivirus*, and the Unclassified genus, and includes numerous important human and animal pathogens. The most common pathogens of the genus *Flavivirus* are Tick-borne encephalitis viruses, Dengue virus (DENV), Yellow fever virus (YFV), West Nile virus (WNV) and Zika virus (ZIKV) and are transmitted mainly by arthropods. YFV is transmitted by the mosquitoes *Aedes aegypti* and *Haemagogus leucocelaenus*. The treatment and management of flaviviruses' infection is not 100% effective, even in cases where vaccines are available. It is thus highly important to study these viruses in terms of their genetic material and mechanisms of infection and reproduction in order

to find efficient ways for their constrain in case of an outbreak (Best, 2016).

The small, enveloped virions of the different members of the *Flaviviridae* family contains a single-stranded, positive-sense RNA genome of about 9.5–12.5 kb. Their genome consists of a single, long open reading frame (ORF), flanked by untranslated regions (UTRs) at 5' and 3' ends. Extensive studies on sub-genomic *Flavivirus* RNA replicons have revealed that the non-structural (NS) proteins, which are encoded by the C-terminal part of the polyprotein, play a crucial role in viral RNA replication. Accordingly, these proteins are assumed to form replication complexes in conjunction with genomic RNA and possibly with other cellular factors (Best, 2016; Chambers *et al.*, 1990). Inhibition of viral proteins, mainly NS3 helicase and NS5 polymerase,

Article history

Received: 05 November 2021

Accepted: 12 November 2021

Published: 07 July 2022

© 2022 Papakonstantinou *et al.*; the authors have retained copyright and granted the Journal right of first publication; the work has been simultaneously released under a Creative Commons Attribution Licence, which allows others to share the work, while acknowledging the original authorship and initial publication in this Journal. The full licence notice is available at <http://journal.embnet.org>.

is becoming increasingly popular (Papageorgiou *et al.*, 2016; Vlachakis, 2021). More specifically, the NS3 protein is a multifunctional polypeptide and encodes three enzymes with different functions including a serine protease, a NTPase and an RNA helicase. The RNA helicase is encoded by the C-terminal domain of the NS3 protein (aa 180-618) and belongs to the helicase superfamily 2 (SF2). Its structure consists of three subdomains, where subdomains 1 and 2 contain eight conserved motifs essential for RNA binding, ATP hydrolysis and structural stability (Fairman-Williams *et al.*, 2010; Pyle, 2008) adopting the RecA-like fold (Rao and Rossmann, 1973), and subdomain 3 forms the single-stranded RNA binding tunnel. Subdomain 3 also mediates the interaction between NS3 and NS5, and the disruption of this interaction is also considered a powerful and effective strategy for designing antiviral compounds (Tay *et al.*, 2015). Viruses carrying an impaired NS3 helicase gene cannot reproduce properly, proving the essential role of NS3 helicase activity in virus replication.

Viral helicase activity is essential for the virus during its reproductive process. NS3 protein appears to be a potential pharmacological target for inhibiting YFV replication (García *et al.*, 2017) and antiviral strategies aiming for flavivirus helicase inhibition has been implemented in various cases (Lim *et al.*, 2013; Luo *et al.*, 2015). Although rare reports of NS3 helicase inhibitors have been reported to date, the presence of halogenated benzenes that inhibit WNV helicase (Sampath and Padmanabhan, 2009) and ivermectin, an antiparasitic drug for helminths, that inhibits JEV and YFV helicases, are reported (Lai *et al.*, 2017; Mastrangelo *et al.*, 2012). In addition, ST-610 and suramin have been reported as DENV helicase inhibitors (Basavannacharya and Vasudevan, 2014; Lim *et al.*, 2013). Compound ML283, which has been shown to act as an inhibitor of HCV and DENV helicases and pyrrolone, acts as a helicase inhibitor for both DENV and WNV (Sweeney *et al.*, 2015). Although increasingly more studies are being conducted at the development of inhibitors for viral helicases, the lack of specific pockets in RNA and NTP binding sites poses a significant problem in the process as significant toxicity may occur, as compounds targeting these sites may also target many similar cellular proteins with helicase or NTPase functions. In addition, another problem in the development of high affinity and potency inhibitors is the inherent flexibility of motor proteins, however allosteric inhibition still remains an attractive idea for inhibitor design (Li *et al.*, 2013). In conclusion, to date no helicase inhibitor has been approved for clinical usage, which may be due to the above limitations in the process of *in-silico* drug development.

Sequence alignments of the Yellow Fever viral helicase identified several conserved sequence motifs that are important for biological functions. So far, the crystal structures of helicases from various RNA viruses have been determined, including the helicases from Yellow Fever Virus (Wu *et al.*, 2005), Hepatitis C virus

(Yao *et al.*, 1997), Dengue virus (Luo *et al.*, 2008a), Zika virus (Tian *et al.*, 2016), and Kunjin virus (Mastrangelo *et al.*, 2007). In the present work, the three-dimensional structure of the helicase enzyme of Yellow Fever virus in complex with a ssRNA molecule was predicted through comparative modelling and a 3D pharmacophore was developed in order to scan and detect specific helicase inhibitors with antiviral potential.

Methods

Sequence Alignment and Phylogenetic Analysis

The amino acid sequence of Yellow Fever viral helicase was obtained from the GenBank database (accession no.: NC_002031, entry name: Yellow Fever virus, complete genome). All available sequences of *Flaviviridae* NS3s were collected from the NIAID Virus Pathogen Database and Analysis Resource (ViPR) (Pickett *et al.*, 2011) and the NCBI RefSeq database. Representative sequences were selected and sequence alignment was performed using the ClustalO algorithm in the Jalview program (Waterhouse *et al.*, 2009a). The phylogenetic trees were constructed with the Neighbor Joining algorithm (Saitou and Nei, 1987) and visualization was performed using iTol¹ and Jalview software (Waterhouse *et al.*, 2009b).

Energy Minimisation

Initially, available structures of *Flaviviridae* helicases were queried in the RSCB Protein Data Bank and a total of 110 structures were identified. 17 representative structures from each species were selected and structural studies were performed to optimize and evaluate the three-dimensional (3D) structure of the X-ray determined YFV helicase (PDB ID: 1YKS) and the other viral helicase structures. Energy minimization was used to remove any residual geometrical strain in each molecular system, using the CHARMM27 forcefield (Foloppe and MacKerell, 2000). Sequence alignments and structural superpositions were performed using the ClustalO algorithm (Sievers *et al.*, 2011) and the MOE software (Group, 2019) respectively.

Molecular electrostatic potential (MEP)

Electrostatic potential surfaces were calculated by solving the nonlinear Poisson–Boltzmann equation using the finite difference method as implemented in the PyMOL Software (Schrödinger, 2020). The potential was calculated on grid points per side (65, 65, 65) and the grid fill by solute parameter was set to 80%. The dielectric constants of the solvent and the solute were set to 80.0 and 2.0, respectively. An ionic exclusion radius of 2.0 Å, a solvent radius of 1.4 Å and a solvent ionic strength of 0.145 M were applied. Amber99 charges and atomic radii were used for this calculation.

¹<https://itol.embl.de>

Model Optimization

Energy minimization was done in MOE initially using the CHARMM27 forcefield (Foloppe and MacKerell, 2000) implemented into the same package, up to a RMSD gradient of 0.0001 to remove the geometrical strain. The model was subsequently solvated with SPC water using the truncated octahedron box extending to 7 Å from the model and molecular dynamics were performed after that at 300K, 1 atm with 2 second step size and for a total of ten nanoseconds, using the NVT ensemble in a canonical environment. NVT stand for Number of atoms, Volume and Temperature that remain constant throughout the calculation. The results of the molecular dynamics simulation were collected into a database by MOE and can be further analyzed.

Model Evaluation

The produced models were initially evaluated within the MOE package (Group, 2019) by a residue packing quality function, which depends on the number of buried non-polar side chain groups and on hydrogen bonding.

High-Throughput Virtual Screening and in-silico de novo drug design

A 3D pharmacophore model was constructed using the Pharmacophore tool in MOE (Group, 2019) and representative pharmacophoric features were selected based on the ssRNA-helicase interactions. High-throughput virtual screening simulations were consequently performed using the pharmacophore query tool in MOE. Novel molecules were *in-silico* designed based on the chemical structures of the WO/2009/125191 patent for HCV helicase inhibitors as scaffolds using the MOE BREED module and were consequently *in-silico* evaluated based on their binding free energies.

Results and Discussion

Description of the Yellow Fever virus helicase structure

The Yellow Fever virus helicase model exhibits the structural features of known *Flaviviridae* helicases, and its structure has been experimentally determined by Wu *et al.* at 1.80Å resolution. Namely, the three distinct domains of helicases as well as the various motifs are structurally similar. The GxGKT/S motif in domain 1 is one of the most crucial motifs in *Flaviviridae* helicases, which is conserved to the same loop in kinases. It is a Walker A motif and binds the β-phosphate of ATP (Saraste *et al.*, 1990). The importance of this motif is highlighted in site directed mutagenesis studies by the fact that the mutant protein is inactive. Furthermore, the DExH motif is another crucial motif for the helicase function, which is responsible for the binding of the Mg²⁺-ATP substrate. According to studies in adenylate and thymidine kinases, an aspartate (Asp170) has been

revealed that binds the Mg²⁺ helping in the establishment of the ATP optimum orientation for nucleophilic attack (Ruff *et al.*, 1991). Finally, QRxGRxGR motif is also a crucial motif, the role of which is exceptionally crucial to the *Flaviviridae* helicase function as it is involved in nucleic acid binding (Gross and Shuman, 1996; Vlachakis, 2009).

The *Flaviviridae* helicases have three domains in total, which are separated by two channels. The first and third domains are more interacting together in contrast with domain two. During the unwinding of double-stranded nucleic acids, domain two undergoes significant movements compared to the other two domains. The channel between domains 3 and 1-2 accommodate the ssRNA during the viral unwinding process. The second domain contains an arginine-rich site where RNA binds to the helicase. The ATP and ssRNA sites were found to have been conserved on the Yellow Fever Virus helicase model (Luo *et al.*, 2008b).

Comparative Modelling

The NS3 domain of *Flaviviridae* contains both the protease and the helicase coding regions. For this study, all available helicase structures of the *Flaviviridae* family were retrieved and filtered to remove redundant and duplicate structures (17 out of 110 in total) and were consequently minimized to remove geometrical strains in each molecular system. The optimized structures were aligned and superposed against the Yellow Fever virus helicase sequence. All the major helicase motifs, characteristic of the *Flaviviridae* family (Garg *et al.*, 2013) were found to be conserved both in sequence and structure and the constructed phylogenetic tree represents the relations between these viral species (Figure 1).

The overall alignment showed a sequence identity that ranged from 18.2% (HCV helicase, PDB ID: 1A1V) to 50.0% (Dengue virus 4 helicase, PDB ID: 5XC6), whereas sequence similarity of the sequences ranged from 28.4% to 66.8%, respectively. The alpha-carbon structural superposition of the *Flaviviridae* helicases against the Yellow Fever helicase exhibited major differences in their domain orientations and features and the resulting RMSD ranged from 1.663 Å to 7.970 Å. The most similar structures identified were the flavivirus helicases of Zika virus (PDB ID: 5MFX) and Dengue virus 4 (PDB ID: 5XC6) (Figure 2).

To construct the ssRNA-helicase complex of the Yellow Fever virus, three available *Flaviviridae* helicase-ssRNA complexes were used as templates (HCV PDB ID:1A1V; ZV PDB ID:5MFX; DV4 PDB ID:5XC6). The coordinates of the ssRNA substrates were transferred to the Yellow Fever helicase structure according to the superposed structures and the three resulting model complexes were evaluated. The models were subjected to energy minimization and molecular dynamics (MD) simulations in the presence of the ssRNA substrate. Based on structural stability and superposition of the consequent binding sites, the Zika virus helicase-

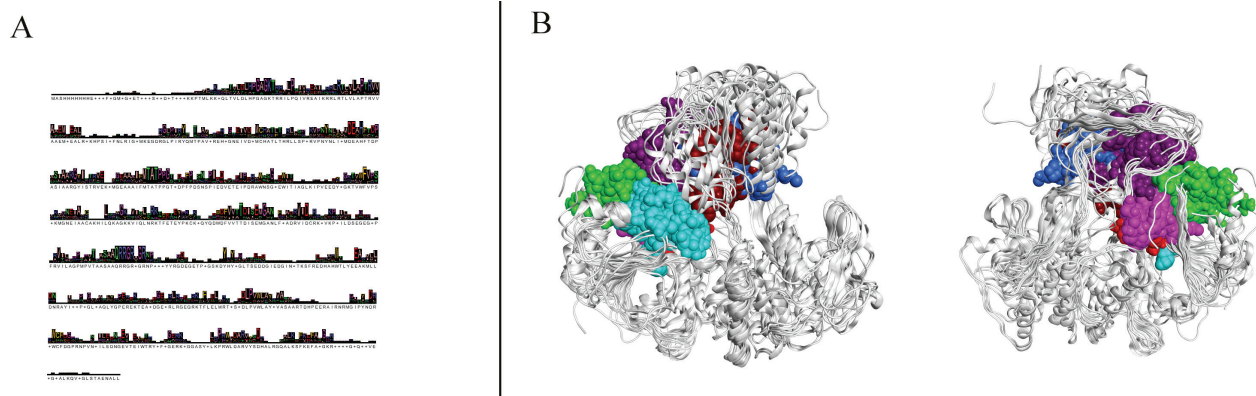


Figure 1. A: Sequence alignment between the representative Flaviviridae helicase sequences where all seven motifs are identified. **B:** A representative phylogenetic tree of the Flaviviridae helicase enzymes. **C:** Structural superposition of the 3-D structures of the representative Flaviviridae helicase enzymes. All seven major conserved motifs of Flaviviridae helicases have been color-coded and represented in CPK format.

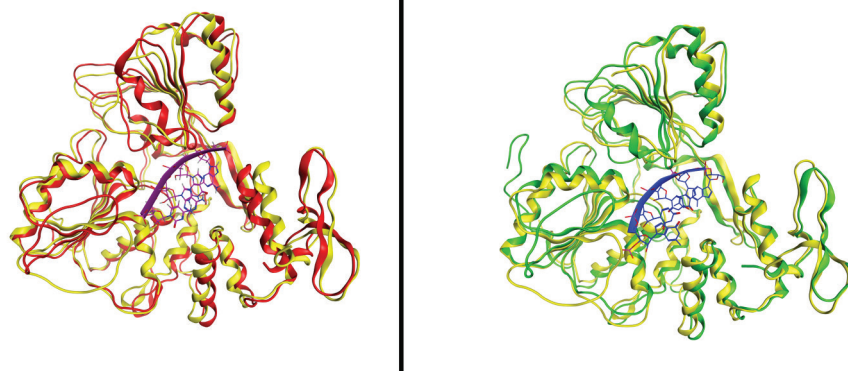


Figure 2. A: The Yellow Fever virus helicase in yellow (PDB ID: 1YKS) superimposed with the Zika virus helicase in red (PDB ID: 5MFX) and the ssRNA substrate in magenta. **B:** The Yellow Fever virus helicase in yellow (PDB ID: 1YKS) superimposed with the Dengue virus 4 helicase in green (PDB ID: 5XC6) and the ssRNA substrate in blue.

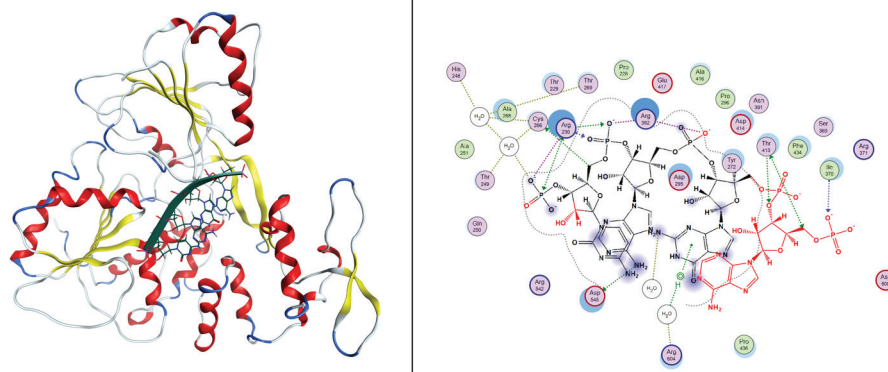


Figure 3. The Yellow Fever helicase-ssRNA complex model. A: The 3-D model of the YF helicase in cartoon representation color coded by structural elements, with the modelled ssRNA fragment in ribbon and stick representation in dark green. **B:** The interaction map of the per-residue ssRNA interaction pattern from Ligplot for Yellow Fever virus helicase.

ssRNA complex was chosen as the most appropriate template (Figure 3). Invariant residues of numerous motifs in the vicinity of the substrate in the Zika virus template structure were conserved in the Yellow Fever virus helicase structural model. Interactions of Yellow Fever helicase-ssRNA fragment were established with

the backbone of the ssRNA fragment, that create non-specific protein–nucleic acid interactions. The bases in the middle of the ssRNA do not appear to interact with the protein. The contacts of the enzymatic receptor emerge mostly from domains one and two of the Yellow Fever helicase and, specifically, from loops between secondary

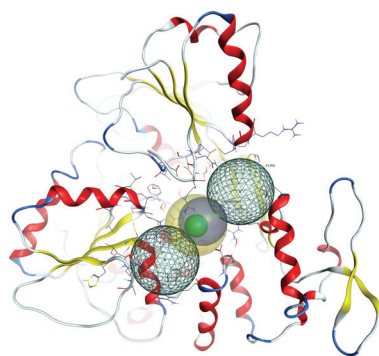


Figure 4. The pharmacophore model for the RNA binding site of the Yellow Fever helicase structure. 5 pharmacophoric sites are represented, two projected ring features in both ends of the channel in dark green mesh, and three dynamic sites in the center of the channel, one aromatic or hydrophobic centroid feature in light green sphere, one site of H-donor or H-acceptor in blue sphere, and one site of H-bond or anion feature in yellow sphere.

structure elements of the latter domains. LigPlot, which is a built-in module of MOE, was used for the drawing of more detailed (i.e. per residue) comparison of the ssRNA interaction pattern between the Yellow Fever virus helicase model and the Zika virus helicase structure.

The Yellow Fever virus helicase-ssRNA model reached a conformational equilibrium similar to that of Zika virus complex based on the 10ns MD simulations revealed. Thus, the viability of the comparative modelling of the Yellow Fever complex model was illustrated by these observations. The Yellow Fever complex model was compared with its template structure by calculating the root mean square deviations (RMSD) between equivalent atoms for the full MD course for evaluation. Large values of RMSD are indicative of systems of poor quality. The C α RMSD of the Yellow Fever virus helicase model from the equivalent domains of the template structures was less than 0.65. This low value of RMSD reflected the high similarity of this structures since it seems to remain conformationally close to the template structure upon the minimization and the molecular dynamics simulation course that followed.

The electrostatic potential surface was calculated to analyze the molecular surface of the simulated Yellow Fever virus complex. In order to compare directly the template structure used in this study, electrostatic potential surfaces were also calculated for the Zika virus helicase. According to the results, the two helicases exhibited almost identical electrostatic surfaces and shared common features such as a negatively charged ssRNA entrance to the helicase tunnel verifying the validity of the model, which was found to share a similar electrostatic surface to its X-ray crystal structure complex template.

Pharmacophore modelling and in-silico de novo drug design

Following the establishment of the YFV helicase-ssRNA model, the specific molecular interactions and physicochemical properties of the complex were analyzed. Based on the interactions identified, a 3-D dynamic pharmacophore model was created, to represent the interaction sites and nucleotide binding channel (Figure 4). The pharmacophore consists of 5 sites representing two projected ring features, one site that represents an annotation of aromatic or hydrophobic centroid feature, one site of H-donor or acceptor feature, and one site of H-bond or anion features. The aromatic ring features are located at the edges of the binding site, whereas the rest of the features are found in the core of the channel. Novel compounds were *in-silico* designed based on evaluated molecules included in the WO/2009/125191 patent, that encompasses molecular structures suitable for use in the treatment of HCV infection against the viral helicase. These compounds are symmetrical in their chemical structure and features accounting for the non-directionality of the nucleotide substrates. Based on their features and interaction properties, these molecules were used as scaffolds in the MOE BREED module and novel structures were generated. The module implements the crossover operator of genetic algorithms by evaluating important features of the original structures and combines fragments to produce novel new energy structures with similar orientation. The designed structures preserve significant intramolecular interactions of the lead compounds. Based on the pharmacophoric representation of the binding site, the collection of the in-house maintained designed compounds were evaluated based on the London dG scoring function of the free energy of binding for each ligand. The pharmacophore-based high-throughput virtual screening identified top compounds that could act as bioactive inhibitors of the YFH helicase, disrupting the binding of single stranded RNA and obstructing the enzyme function.

Conclusions

Computer-based methodologies have become an integral part of the process of developing new drugs and repurposing of approved drugs against numerous diseases, as well as discover potential pharmacological targets. Developed applications for computational drug design are continuously upgrading and transforming traditional methodologies and pipelines, speeding up the research in antiviral strategies. In contrast to the traditional drug development methods which are time consuming and costly, computational drug design methods are widely used in the development of antivirals (Shaker *et al.*, 2021). These state-of-the-art techniques dock small molecules into macromolecular targets and predict the affinity and activity of small molecules (Dalkas *et al.*, 2012). Interestingly, information technologies

Table 1. Smiles representation and London dG scoring values for the top 10 novel designed molecules.

mol	smiles	London dG
1	<chem>O=C(Nc1ccc(-c2[nH]c3c(n2)cccc3)cc1)c1c(-c2ccc(-c3[nH]c4c(n3)cccc4)cc2)cc(C(=O)Nc2ccc(-c3[nH]c4c(n3)cccc4)cc2)cc1</chem>	-7.6665
2	<chem>O=C(Nc1cc(-c2[nH]c3c(n2)cccc3)c(-c2[nH]c3c(n2)cccc3)cc1)CCCCC(=O)Nc1ccc(-c2[nH]c3c(n2)cccc3)cc1</chem>	-6.9248
3	<chem>O=C(Nc1ccc(-c2[nH]c3c(n2)cccc3)cc1)c1c(-c2ccc(-c3[nH]c4c(n3)cccc4)cc2)cc(-c2ccc(C(=O)Nc3ccc(-c4[nH]c5c(n4)cccc5)cc3)cc2)cc1</chem>	-6.0711
4	<chem>O=C(Nc1ccc(-c2[nH]c3c(n2)cccc3)cc1)CCCCCCCCNc1ccc(-c2[nH]c3c(n2)cccc3)cc1</chem>	-6.0541
5	<chem>O=C(Nc1ccc(-c2[nH]c3c(n2)cccc3)cc1)CCCCCCCCC(=O)N</chem>	-5.9514
6	<chem>O=C(Nc1ccc(-c2[nH]c3c(n2)cccc3)cc1)CC[C@H]1[C@H](C(=O)Nc2ccc(-c3[nH]c4c(n3)cccc4)cc2)CCCC1</chem>	-5.6812
7	<chem>O=C(Nc1ccc(-c2[nH]c3c(n2)cccc3)cc1)C(=O)c1ccc(C(=O)Nc2ccc(-c3[nH]c4c(n3)cccc4)cc2)cc1</chem>	-5.4822
8	<chem>O=C(Nc1ccc(-c2[nH]c3c(n2)cccc3)cc1)CCCCC1c(NC(=O)c2c(C(=O)Nc3ccc(-c4[nH]c5c(n4)cccc5)cc3)cccc2)ccc(-c2[nH]c3c(n2)cccc3)c1</chem>	-5.4674
9	<chem>O=C(Nc1ccc(-c2[nH]c3c(n2)cccc3)cc1)CCCCCCCC=O</chem>	-5.4051
10	<chem>O=C(Nc1ccc(-c2[nH]c3c(n2)cccc3)cc1)c1ccc(C(=O)c2ccc(-c3[nH]c4c(n3)cccc4)cc2)cc1</chem>	-5.3922

and machine learning algorithms are almost inevitably implemented in these new approaches to improve the efficacy of the prediction.

Especially nowadays that we are going through a period of public health crisis due to the SARS-CoV-2 virus, the need to develop a quick and efficient pipeline for identifying potential antiviral drugs for future health risks is imperative (Basu *et al.*, 2021). Members of the *Flaviviridae* family, are already endemic to African and South American countries. In addition, several cases of *Flaviviridae* outbreaks are being reported in Southern Europe and America (WHO, 7 May 2019). Numerous studies are being performed to detect effective drug targets in several viruses of this family, with nonstructural proteins, such as the viral protease, helicase and polymerase enzymes, being among the most prominent pharmacological targets (Vlachakis, 2021). Thus, computational methods for homology modelling and prediction of viral protein structures, such as bovine viral diarrhea virus (BVDV) (Xu *et al.*, 1997), Classical Swine Fever virus (Li *et al.*, 2018), Dengue virus and Zika virus (Ekins *et al.*, 2016; Jain *et al.*, 2016), are used to develop new promising viral inhibitors.

In this study, the three-dimensional structure of the Yellow Fever virus helicase in complex with a single stranded RNA molecule was established based on available templates of helicase enzymes cocrystallized with ssRNA of the *Flaviviridae* family. An extensive comparative analysis was performed and the produced model using the structure of Zika virus helicase as template was optimized. The evaluation of the model was carried out successfully in terms of geometry, fold recognition as well as in terms of the criteria required for members of the viral *Flaviviridae* family. In addition, the Yellow Fever virus complex model was evaluated by molecular dynamics simulations and used to design a 3-D pharmacophore, indicative of the RNA binding site

properties. Novel chemical structures were designed through an *in-silico* approach that combines significant features of evaluated structures against viral helicases through the implementation of genetic algorithms. A pharmacophore-based screening was performed, and potent molecules were evaluated and recognized as potential inhibitors of the activity of the Yellow Fever virus helicase. Our applied methodology is paving the way towards the designing and more efficient screening of potential novel modulator compounds against the YFV, as well as attest and designate the NS3 helicase as an antiviral pharmacological target of uttermost value and potential.

Key Points

- Yellow Fever is a viral hemorrhagic with high mortality rates.
- Designing and screening for a potential novel modulator against the YFV helicase is of great value.
- A rational structure-based drug design was performed for the evaluation of YFV helicase inhibitors.
- Computer-based methodologies are an integral part of the process of novel drug development and the discovery of potential pharmacological targets.

Funding

This work is funded by the ESPA Young Researchers Support, «Rational Drug Design of Novel Antiviral Agents against the Helicase Enzyme of the Yellow Fever Virus», MIS 5048546, NSRF 2014 – 2020.

References

- Basavannacharya C and Vasudevan SG (2014) Suramin inhibits helicase activity of NS3 protein of dengue virus in a fluorescence-based high throughput assay format. *Biochem Biophys Res Commun* **453**(3), 539-544. <http://dx.doi.org/10.1016/j.bbrc.2014.09.113>

- Basu S, Ramaiah S and Anbarasu A (2021) In-silico strategies to combat COVID-19: A comprehensive review. *Biotechnol Genet Eng Rev* **37**(1), 64-81. <http://dx.doi.org/10.1080/02648725.2021.1966920>
- Best SM (2016) Flaviviruses. *Curr Biol* **26**(24), R1258-r1260. <http://dx.doi.org/10.1016/j.cub.2016.09.029>
- Chambers TJ, Hahn CS, Galler R and Rice CM (1990) Flavivirus genome organization, expression, and replication. *Annu Rev Microbiol* **44**, 649-688. <http://dx.doi.org/10.1146/annurev.mi.44.100190.003245>
- Dalkas GA, Vlachakis D, Tzagkrasoulis D, Kastania A and Kossida S (2012) State-of-the-art technology in modern computer-aided drug design. *Briefings in Bioinformatics* **14**(6), 745-752. <http://dx.doi.org/10.1093/bib/bbs063>
- Ekins S, Liebler J, Neves BJ, Lewis WG, Coffee M *et al.* (2016) Illustrating and homology modeling the proteins of the Zika virus. *F1000Res* **5**, 275. <http://dx.doi.org/10.12688/f1000research.8213.2>
- Fairman-Williams ME, Guenther U-P and Jankowsky E (2010) SF1 and SF2 helicases: family matters. *Current Opinion in Structural Biology* **20**(3), 313-324. <http://dx.doi.org/https://doi.org/10.1016/j.sbi.2010.03.011>
- Foloppe N and MacKerell A (2000) All-atom empirical force field for nucleic acids: I. Parameter optimization based on small molecule and condensed phase macromolecular target data. *Journal of Computational Chemistry* **21**, 86-104. [http://dx.doi.org/10.1002/\(SICI\)1096-987X\(20000130\)21:2%3C86::AID-JCC2%3E3.0.CO;2-G](http://dx.doi.org/10.1002/(SICI)1096-987X(20000130)21:2%3C86::AID-JCC2%3E3.0.CO;2-G)
- García LL, Padilla L and Castaño JC (2017) Inhibitors compounds of the flavivirus replication process. *Virol J* **14**(1), 95. <http://dx.doi.org/10.1186/s12985-017-0761-1>
- Garg H, Lee RTC, Tek NO, Maurer-Stroh S and Joshi A (2013) Identification of conserved motifs in the West Nile virus envelope essential for particle secretion. *BMC Microbiology* **13**(1), 197. <http://dx.doi.org/10.1186/1471-2180-13-197>
- Gross CH and Shuman S (1996) The QRxGRxGRxxxG motif of the vaccinia virus DEXH box RNA helicase NPH-II is required for ATP hydrolysis and RNA unwinding but not for RNA binding. *J Virol* **70**(3), 1706-1713. <http://dx.doi.org/10.1128/jvi.70.3.1706-1713.1996>
- Group CC (2019) Molecular Operating Environment (MOE). 1010 Sherbooke St. West, Suite #910, Montreal, QC, Canada, H3A 2R7, 2021.
- Jain R, Coloma J, García-Sastre A and Aggarwal AK (2016) Structure of the NS3 helicase from Zika virus. *Nat Struct Mol Biol* **23**(8), 752-754. <http://dx.doi.org/10.1038/nsmb.3258>
- Lai JH, Lin YL and Hsieh SL (2017) Pharmacological intervention for dengue virus infection. *Biochem Pharmacol* **129**, 14-25. <http://dx.doi.org/10.1016/j.bcp.2017.01.005>
- Li K, Frankowski KJ, Hanson AM, Ndjomou J, Shanahan MA *et al.* (2013) Hepatitis C virus NS3 helicase inhibitor discovery. *Probe Reports from the NIH Molecular Libraries Program* [Internet].
- Li W, Wu B, Soca WA and An L (2018) Crystal Structure of Classical Swine Fever Virus NS5B Reveals a Novel N-Terminal Domain. *J Virol* **92**(14). <http://dx.doi.org/10.1128/jvi.00324-18>
- Lim SP, Wang QY, Noble CG, Chen YL, Dong H *et al.* (2013) Ten years of dengue drug discovery: progress and prospects. *Antiviral Res* **100**(2), 500-519. <http://dx.doi.org/10.1016/j.antiviral.2013.09.013>
- Luo D, Vasudevan SG and Lescar J (2015) The flavivirus NS2B-NS3 protease-helicase as a target for antiviral drug development. *Antiviral Res* **118**, 148-158. <http://dx.doi.org/10.1016/j.antiviral.2015.03.014>
- Luo D, Xu T, Hunke C, Grüber G, Vasudevan SG *et al.* (2008a) Crystal structure of the NS3 protease-helicase from dengue virus. *J Virol* **82**(1), 173-183. <http://dx.doi.org/10.1128/JVI.01788-07>
- Luo D, Xu T, Watson RP, Scherer-Becker D, Sampath A *et al.* (2008b) Insights into RNA unwinding and ATP hydrolysis by the flavivirus NS3 protein. *Embo j* **27**(23), 3209-3219. <http://dx.doi.org/10.1038/emboj.2008.232>
- Mastrangelo E, Milani M, Bollati M, Selisko B, Peyrane F *et al.* (2007) Crystal structure and activity of Kunjin virus NS3 helicase; protease and helicase domain assembly in the full length NS3 protein. *J Mol Biol* **372**(2), 444-455. <http://dx.doi.org/10.1016/j.jmb.2007.06.055>
- Mastrangelo E, Pezzullo M, De Burghgraeve T, Kaptein S, Pastorino B *et al.* (2012) Ivermectin is a potent inhibitor of flavivirus replication specifically targeting NS3 helicase activity: new prospects for an old drug. *J Antimicrob Chemother* **67**(8), 1884-1894. <http://dx.doi.org/10.1093/jac/dks147>
- Pickett BE, Sadat EL, Zhang Y, Noronha JM, Squires RB *et al.* (2011) ViPR: an open bioinformatics database and analysis resource for virology research. *Nucleic Acids Research* **40**(D1), D593-D598. <http://dx.doi.org/10.1093/nar/gkr859>
- Pyle AM (2008) Translocation and unwinding mechanisms of RNA and DNA helicases. *Annu Rev Biophys* **37**, 317-336. <http://dx.doi.org/10.1146/annurev.biophys.37.032807.125908>
- Rao ST and Rossmann MG (1973) Comparison of super-secondary structures in proteins. *Journal of Molecular Biology* **76**(2), 241-256. [http://dx.doi.org/10.1016/0022-2836\(73\)90388-4](http://dx.doi.org/10.1016/0022-2836(73)90388-4)
- Ruff M, Krishnaswamy S, Boeglin M, Poterszman A, Mitschler A *et al.* (1991) Class II aminoacyl transfer RNA synthetases: crystal structure of yeast aspartyl-tRNA synthetase complexed with tRNA(Asp). *Science* **252**(5013), 1682-1689. <http://dx.doi.org/10.1126/science.2047877>
- Saitou N and Nei M (1987) The neighbor-joining method: a new method for reconstructing phylogenetic trees. *Molecular Biology and Evolution* **4**(4), 406-425. <http://dx.doi.org/10.1093/oxfordjournals.molbev.a040454>
- Sampath A and Padmanabhan R (2009) Molecular targets for flavivirus drug discovery. *Antiviral Res* **81**(1), 6-15. <http://dx.doi.org/10.1016/j.antiviral.2008.08.004>
- Saraste M, Sibbald PR and Wittinghofer A (1990) The P-loop - a common motif in ATP- and GTP-binding proteins. *Trends Biochem Sci* **15**(11), 430-434. [http://dx.doi.org/10.1016/0968-0004\(90\)90281-f](http://dx.doi.org/10.1016/0968-0004(90)90281-f)
- Schrödinger L, & DeLano, W. (2020). "PyMOL." from <http://www.pymol.org/pymol>
- Shaker B, Ahmad S, Lee J, Jung C and Na D (2021) In silico methods and tools for drug discovery. *Comput Biol Med* **137**, 104851. <http://dx.doi.org/10.1016/j.compbiomed.2021.104851>
- Sievers F, Wilm A, Dineen D, Gibson TJ, Karplus K *et al.* (2011) Fast, scalable generation of high-quality protein multiple sequence alignments using Clustal Omega. *Mol Syst Biol* **7**, 539. <http://dx.doi.org/10.1038/msb.2011.75>
- Sweeney NL, Hanson AM, Mukherjee S, Ndjomou J, Geiss BJ *et al.* (2015) Benzothiazole and Pyrrolone Flavivirus Inhibitors Targeting the Viral Helicase. *ACS Infect Dis* **1**(3), 140-148. <http://dx.doi.org/10.1021/id5000458>
- Tay MYF, Saw WG, Zhao Y, Chan KWK, Singh D *et al.* (2015) The C-terminal 50 Amino Acid Residues of Dengue NS3 Protein Are Important for NS3-NS5 Interaction and Viral Replication*. *Journal of Biological Chemistry* **290**(4), 2379-2394. <http://dx.doi.org/10.1074/jbc.M114.607341>
- Tian H, Ji X, Yang X, Xie W, Yang K *et al.* (2016) The crystal structure of Zika virus helicase: basis for antiviral drug design. *Protein Cell* **7**(6), 450-454. <http://dx.doi.org/10.1007/s13238-016-0275-4>
- Vlachakis D (2009) Theoretical study of the Usutu virus helicase 3D structure, by means of computer-aided homology modelling. *Theoretical Biology and Medical Modelling* **6**(1), 9. <http://dx.doi.org/10.1186/1742-4682-6-9>
- Vlachakis D (2021) Genetic and structural analyses of ssRNA viruses pave the way for the discovery of novel antiviral pharmacological targets. *Molecular Omics* **17**(3), 357-364. <http://dx.doi.org/10.1039/D0MO00173B>
- Waterhouse AM, Procter JB, Martin DM, Clamp M and Barton GJ (2009a) Jalview Version 2--a multiple sequence alignment editor and analysis workbench. *Bioinformatics* **25**(9), 1189-1191. <http://dx.doi.org/10.1093/bioinformatics/btp033>

- Waterhouse AM, Procter JB, Martin DMA, Clamp M and Barton GJ (2009b) Jalview Version 2—a multiple sequence alignment editor and analysis workbench. *Bioinformatics* **25**(9), 1189-1191. <http://dx.doi.org/10.1093/bioinformatics/btp033>
- WHO (7 May 2019). “Yellow fever” from <https://www.who.int/news-room/fact-sheets/detail/yellow-fever>.
- Wu J, Bera AK, Kuhn RJ and Smith JL (2005) Structure of the Flavivirus helicase: implications for catalytic activity, protein interactions, and proteolytic processing. *J Virol* **79**(16), 10268-10277. <http://dx.doi.org/10.1128/jvi.79.16.10268-10277.2005>
- Xu J, Mendez E, Caron PR, Lin C, Murcko MA *et al.* (1997) Bovine viral diarrhea virus NS3 serine proteinase: polypeptide cleavage sites, cofactor requirements, and molecular model of an enzyme essential for pestivirus replication. *J Virol* **71**(7), 5312-5322. <http://dx.doi.org/10.1128/jvi.71.7.5312-5322.1997>
- Yao N, Hesson T, Cable M, Hong Z, Kwong AD *et al.* (1997) Structure of the hepatitis C virus RNA helicase domain. *Nat Struct Biol* **4**(6), 463-467. <http://dx.doi.org/10.1038/nsb0697-463>